Table 9-2 (Continued-2) Evaluation of Antibody Production by Recombinant Human Granulocyte Macrophage Colony-Stimulating Factor (GM-CSF) Product in Cynomolgus Monkeys: II
Bone marrow examinations (males)

Day 92

Group	Dose level	Animal No.	Myeloid cells (10^4/μL)										MONO	LYMPH	PLASM	MEGK	RETICU	MACRO	MAST	OTHERS
			MBL	PRO	N MY	N META	N BAND	N SEG	EOS	BASO	MIT M	Total	(10^4/μL)	(10^4/μL)	(10^4/μL)	(10^4/μL)	(10^4/μL)	(10^4/μL)	(10^4/μL)	(10^4/μL)
I CHO cell-derived GM-CSF	15 μg/body	UJM01	1.0	3.2	7.8	9.1	22.4	29.5	4.2	0.3	1.0	78.4	3.9	27.5	1.0	0.3	0.0	1.0	0.0	0.0
		UJM02	0.0	3.5	10.7	6.0	12.4	19.9	5.2	0.6	0.6	58.8	6.3	19.6	0.6	0.3	0.0	0.0	0.0	0.0
II Escherichia coli-derived GM-CSF	15 μg/body	UJM11	0.0	6.2	11.7	8.7	14.3	14.6	1.9	0.6	0.3	58.3	5.5	32.1	1.6	0.3	0.0	1.3	0.3	0.0
		UJM12	0.0	2.3	6.6	8.6	18.2	22.1	2.0	1.0	0.7	61.4	3.3	13.9	1.0	0.3	0.0	1.3	0.0	0.0

厚生労働科学研究費補助金

医療技術実用化総合研究事業（臨床研究・治験推進研究事業）

肺胞蛋白症の吸入治療のための新規 GM-CSF 製剤の非臨床試験

（H24- 臨研推 - 一般 - 003）

平成 26 年度　総括･分担研究報告書

研究成果の刊行物・別冊

（2/2 冊）

研究代表者　田澤 立之

平成 27 (2015) 年 5 月

厚生労働科学研究費補助金

医療技術実用化総合研究事業（臨床研究・治験推進研究事業）

肺胞蛋白症の吸入治療のための新規 GM-CSF 製剤の非臨床試験

（H24-臨研推－一般 - 003）

平成 26 年度　総括・分担研究報告書

研究成果の刊行物・別刷

（2/2 冊）

研究代表者　田澤　立之

平成 27（2015）年 5 月

NOTE *Immunology*

Up-Regulation of Cluster of Differentiation (CD) 11b Expression on the Surface of Canine Granulocytes with Human Granulocyte-Macrophage Colony-Stimulating Factor (GM-CSF)

Kazuhide NAKAGAKI[1)]*, Yuka NUNOMURA[1)], Kanji UCHIDA[2)], Koh NAKATA[3)] and Ryushi TAZAWA[3)]

[1)]*Department of Virology and Immunology, College of Veterinary Medicine, Nippon Veterinary and Animal Science University, Tokyo 180–8602, Japan*
[2)]*Department of Anesthesiology, the University of Tokyo Hospital, Tokyo 113–0033, Japan*
[3)]*Bioscience Medical Research Center, Niigata University Medical and Dental Hospital, Niigata 951–8520, Japan*

(Received 29 January 2014/Accepted 25 April 2014/Published online in J-STAGE 15 May 2014)

ABSTRACT. Granulocyte-macrophage colony-stimulating factor (GM-CSF) is a pleiotropic cytokine, sharing a common beta subunit (CDw131) with interleukins 3 and 5. GM-CSF is important for its direct and indirect involvement in host defense. In veterinary medicine, human (h) GM-CSF has been used as a substitute for canine GM-CSF to stimulate canine granulocytes and macrophages. In this study, we compared the effects of three distinct hGM-CSFs produced by bacteria, yeasts and Chinese hamster ovary (CHO) cells with those of *Escherichia* (E) *coli*-produced canine GM-CSF on the cluster of differentiation 11b (CD11b) expression in canine granulocytes. The median effective dose (ED_{50}) of hGM-CSFs from bacteria, yeasts and CHO cells was 3.09, 4.09 and 4.27 *ng*/m*l*, respectively, with no significant difference among three. In contrast, a significant difference was observed between ED_{50} of canine GM-CSF (0.56 *ng*/m*l*) and three hGM-CSFs according to the paired *t*-test ($P<0.05$). We conclude that hGM-CSF can activate canine granulocytes, but the average activity of the three rhGM-CSFs was approximately 15% of that of canine GM-CSF.

KEY WORDS: canine, CD11b, flow cytometry, granulocyte-macrophage colony-stimulating factor, median fluorescence intensity, xenostimulation

doi: 10.1292/jvms.14-0056: *J. Vet. Med. Sci.* 76(8): 1173–1176, 2014

Human granulocyte-macrophage colony-stimulating factor (hGM-CSF) is a protein of 144 amino acids (AA), including the signal peptide of 18 AA, and is produced by various types of cells. The protein is monomeric, but its active form basically takes a noncovalent homodimmer in nature. Although GM-CSF is a major cytokine for hemopoiesis like granulocyte colony-stimulating factor, macrophage colony-stimulating factor and erythropoietin, the cytokine has been known to be involved in the enhancement of eosinophil chemotaxis [7], maturation of macrophages and dendritic cells [17], granulocyte activation [1], adjuvant effect [3] and inhibition of apoptosis [4].

Cluster of differentiation molecule 11b (CD11b), known as its integrin α M subunit, consists of macrophage-1 antigen (Mac-1) with CD18. The molecule is expressed in many types of cells, and the CD11b expression on the surfaces of granulocytes and macrophages is increased by their activation, playing an important role in host defense. Mac-1 has been reported to support neutrophil immobilization and migration [6] and is also known as complement receptor 3 (CR3) that binds to iC3b, eliminating pathogens and immune complexes by neutrophils, macrophages and the reticuloendothelial system. CD11b is rapidly elevated by the activation of neutrophils and macrophages, and the amount of CD11b in neutrophils correlates with their activation and inflammation [11].

Clinical trials of the adjuvant therapy and the prevention form leukocytopenia with GM-CSF in veterinary cancer medicine have been started, but the preparation of canine GM-CSF for clinical use is still unavailable. Thus, we just have to choose that of human GM-CSF (hGM-CSF) at the present time. Because hGM-CSF is active in canine cells, it has been empirically employed as a substitute for canine GM-CSF [18, 22]; however, its quantitative activity in canine cells has not been elucidated. Here, we compared the effects of hGM-CSF to those of canine GM-CSF in canine granulocytes and also measured the median effective doses (ED_{50}) of three different rhGM-CSFs in canine granulocytes.

Anti-CD11b (M1/70) conjugated with allophycocyanin-Cy7, Gr-1 with allophycocyanin and anti-human CD14 with phycoerythrin were purchased from BioLegend Co., Ltd. (San Diego, CA, U.S.A.; provided by Tomy Digital, Tokyo, Japan). Molgramostim; *Escherichia (E.) coli*-produced recombinant human GM-CSF (rhGM-CSF), sargramostim produced by yeasts and canine recombinant GM-CSF were obtained from Amoytop Biotech (Xiamen, Fujian, People's Republic of China), Genzyme corporation (Cambridge, MA, U.S.A.) and R&D systems (Minneapolis, MN, U.S.A.), respectively. JCR Pharmaceuticals Co., Ltd. (Akashi, Japan) donated rhGM-CSF produced by Chinese hamster ovary (CHO) cells.

*CORRESPONDENCE TO: NAKAGAKI, K., Department of Virology and Immunology, College of Veterinary Medicine, Nippon Veterinary and Animal Science University, 1–7–1 Kyonan, Musashino, Tokyo 180–8602, Japan. e-mail: kazu_nakagaki@hotmail.com

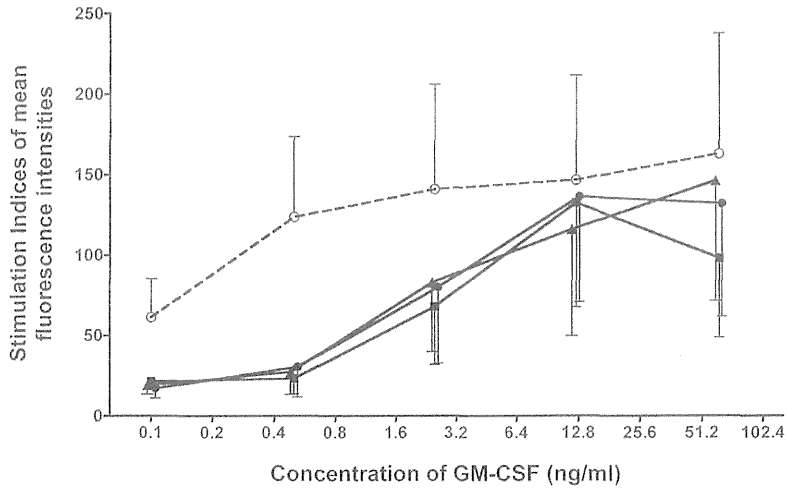

Fig. 1. Dose-response curves of CD11b expression with various granulocyte-macrophage colony-stimulating factors in canine granulocytes. Sigmoid curves represent dose-responses of molgramostim (solid circle), sargramostim (solid square), CHO-produced hGM-CSF (solid triangle) and canine GM-CSF (open circle and broken line). The points and bars show the average values and standard deviations from 4 animals, respectively. X and Y axes show the concentrations of GM-CSF (*ng*/m*l*) and stimulation indices, respectively.

Heparinized canine blood was obtained from 2 male and 2 female beagles for practical trainings of students at Nippon Veterinary and Life Science University. These beagles were individually housed, fed dog chows once a day and drank water *ad libitum*. These bloods were transported to our laboratory and processed at room temperature within 1 hr. Briefly, 100-μl aliquots of the blood were aseptically placed in 2.0-m*l* sterile microtubes, to which various amounts of canine or hGM-CSF were added at final concentrations of 0.02–62.5 *ng*/m*l* or macrophage-serum free medium (macrophage-SFM; Invitrogen Corporation, Carlsbad, CA, U.S.A.) alone. Subsequently, all the samples were incubated for 15 min at a 37°C in a 5% CO_2 incubator without shaking.

After stimulation, antibody cocktail was added to each tube, which was then incubated for 30 min at 4°C. The blood was hemolyzed with 0.15 M ammonium chloride containing 1 mM $KHCO_3$ and 0.1 mM EDTA 4Na (pH 7.3), washed twice with flow cytometer buffer (PBS containing 2% BSA and 0.1% sodium azide) and then fixed in FluoroFix™ buffer (BioLegend), as per the manufacturer's instructions. The cells were re-suspended in 100 μl flow cytometer buffer (PBS containing 2% BSA and 0.05% sodium azide). Data were acquired using FACSArray (BD Bioscience, San Jose, CA, U.S.A.), gating the granulocyte area on a forward vs. side scatter. The median fluorescence intensities (MFIs) of $CD11b^+$ population were obtained under the gate of granulocytes at SSC vs. FSC scatter and $CD14^-$. The indices of MFIs were determined by dividing MFIs from GM-stimulated cultures by MFI from PBS-cultured granulocytes. ED_{50}, determined from MFI values using the probit method, was statistically analyzed using paired *t*-tests at every GM-CSF dose.

Three hGM-CSFs revealed increased CD11b expression on canine granulocytes in a dose-dependent manner (Fig. 1). ED_{50} of molgramostim, sargramostim and hGM-CSF from CHO cells was 3.09, 4.09 and 4.27 *ng*/m*l*, respectively; moreover, no significant difference was observed among these rhGM-CSFs (Table 1). In contrast, ED_{50} of canine rGM-CSF was 0.56 *ng*/m*l*, which was significantly different from the three rhGM-CSFs according to the paired *t*-test results ($P<0.05$). Further, ED_{50} of molgramostim, sargramostim and rhGM-CSF from the CHO cells was 18.1%, 13.7% and 13.1%, respectively, compared with the canine rGM-CSF for canine granulocytes.

GM-CSF is not only an important hemopoietic cytokine, but also involved in the upregulation of the immune system and host-defense [5, 19, 21], because immune cells express its receptor [10, 14]. In experiments using dogs, rhGM-CSF has been employed as a substitute for the canine reagent [2, 16].

GM-CSF activity is usually measured by the proliferation of cells that are GM-CSF-dependent; e.g. TF-1 for hGM-CSF [9]. The detection of augmented CD11b with GM-CSF is rapid and easy. CD11b expression on the surface of neutrophils has been reported to elevate by GM-CSF stimulation [12, 15]. Uchida *et al.* have reported that the quick elevation of CD11b expression on human neutrophils by GM-CSF stimulation was caused by its endogenous molecules but not de novo synthesis [20]. According to a modified Uchida method [20], we detected the activities of rhGM-CSFs in canine neutrophils in a dose-dependent manner. We conclude it may not be a problem to employ rhGM-CSF to canine experiment. This technique doesn't require any GM-CSF-dependent cell line and is applicable to every animal species.

Table 1. Median effective doses of various granulocyte-macrophage colony-stimulating factors in expression of CD11b in canine granulocytes

GM-CSF	ED_{50} (ng/ml)	Specific activities (units/μg)	Relative activities (%) to canine GM-CSF in ED_{50}
Molgramostim	3.09 ± 1.18 [a]	323.6	18.1
Sargramostim	4.09 ± 1.56 [a]	244.5	13.7
CHO hGM-CSF	4.27 ± 1.51 [a]	234.2	13.1
Canine GM-CSF	0.56 ± 0.46 [a]	1,785.7	-

a) Median effective dose (ED_{50}) of canine granulocyte-macrophage colony-stimulating factor (GM-CSF) significantly differed from those of hGM-CSFs according to the paired *t*-test results ($P<0.05$).

Furthermore, it has been reported that some mouse cells are not stimulated by hGM-CSF. However, McClure *et al.* proved that rhGM-CSF activated the BaF-B03 mouse cell line transfected with human GM-CSF receptor α subunit gene [13]. The intracytoplasmic region of the subunit did not participate in the signal transduction [23], which suggests that the α subunit plays an important role in binding species-specifically to GM-CSF. Therefore, the α subunit of canine GM-CSF may have an effective affinity to rhGM-CSF, although rhGM-CSFs had a weaker impact on canine granulocytes compared with canine rGM-CSF in this study. Therefore, to obtain an effect equivalent to an expected activity in dogs with hGM-CSF, we must employ an approximately septuplet dose of rhGM-CSF (Table 1). Nevertheless, this indicates that rhGM-CSF can be a valuable tool for a canine study.

In addition, we also compared GM-CSFs from three different sources: *E. coli*, yeasts and CHO cells; although no significant difference was determined in ED_{50} for the three sources, *E. coli*-produced rhGM-CSF (molgramostim) revealed the highest activity. Moreover, Kelleher *et al.* determined that *E. coli*-produced hGM-CSF had higher efficacy with regard to the proliferation of TF-1 cells compared with that of CHO protein [8]. Although we are not able to explain why molgramostim exhibited the highest activity in our study, Kelleher *et al.* suggested that the difference was the result of the higher affinity of *E. coli* protein [8]. Molgramostim is not much different from the other two types investigated without their glycosylation, which may be involved in their 3-D conformation and homodimmer formation and/or interfere with their interactions with GM-CSFR, affecting GM-CSF activity. Thus, the differences in glycosylation may be responsible for their varied activities.

ACKNOWLEDGMENTS. We thank Ms. Natuko Nogami, a Junior Research Assistant for her technical support. Supported by a grant from the Ministry of Health Labor and Welfare, Japan (H24-Rinkensui-Ippan-003) and in part by the program for the Strategic Research Foundation at Private Universities, 2009–12 of the Japanese Ministry of Education, Culture, Sports, Science and Technology, Tokyo, Japan.

REFERENCES

1. Al-Shami, A. and Naccache, P. H. 1999. Granulocyte-macrophage colony-stimulating factor-activated signaling pathways in human neutrophils. Involvement of jak2 in the stimulation of phosphatidylinositol 3-kinase. *J. Biol. Chem.* **274**: 5333–5338. [Medline] [CrossRef]
2. Bergman, P. J., Camps-Palau, M. A., McKnight, J. A., Leibman, N. F., Craft, D. M., Leung, C., Liao, J., Riviere, I., Sadelain, M., Hohenhaus, A. E., Gregor, P., Houghton, A. N., Perales, M. A. and Wolchok, J. D. 2006. Development of a xenogeneic DNA vaccine program for canine malignant melanoma at the Animal Medical Center. *Vaccine* **24**: 4582–4585. [Medline] [CrossRef]
3. Chen, Q., He, F., Kwang, J., Chan, J. K. and Chen, J. 2012. GM-CSF and IL-4 stimulate antibody responses in humanized mice by promoting T, B, and dendritic cell maturation. *J. Immunol.* **189**: 5223–5229. [Medline] [CrossRef]
4. Choi, J. K., Kim, K. H., Park, H., Park, S. R. and Cho, B. H. 2011. Granulocyte-macrophage colony-stimulating factor shows anti-apoptotic activity in neural progenitor cells via JAK/STAT5-Bcl-2 pathway. *Apoptosis* **16**: 127–134. [Medline] [CrossRef]
5. Fleetwood, A. J., Cook, A. D. and Hamilton, J. A. 2005. Functions of granulocyte-macrophage colony-stimulating factor. *Crit. Rev. Immunol.* **25**: 405–428. [Medline] [CrossRef]
6. Hughes, B. J., Holler, J. C., Crockett-Torabi, E. and Smith, C. W. 1992. Recruitment of CD11b/CD18 to the neutrophil surface and adherence dependent locomotion. *J. Clin. Invest.* **90**: 1687–1696. [Medline] [CrossRef]
7. Kaatz, M., Berod, L., Czech, W., Idzko, M., Lagadari, M., Bauer, A. and Norgauer, J. 2004. Interleukin-5, interleukin-3 and granulocyte-macrophage colony-stimulating factor prime actin-polymerization in human eosinophils: A study with hypodense and normodense eosinophils from patients with atopic dermatitis. *Int. J. Mol. Med.* **14**: 1055–1060. [Medline]
8. Kelleher, C. A., Wong, G. G., Clark, S. C., Schendel, P. F., Minden, M. D. and McCulloch, E. A. 1988. Binding of iodinated recombinant human GM-CSF to the blast cells of acute myeloblastic leukemia. *Leukemia* **2**: 211–215. [Medline]
9. Kitamura, T., Tange, T., Terasawa, T., Chiba, S., Kuwaki, T., Miyagawa, K., Piao, Y. F., Miyazono, K., Urabe, A. and Takaku, F. 1989. Establishment and characterization of a unique human cell line that proliferates dependently on GM-CSF, IL-3, or erythropoietin. *J. Cell. Physiol.* **140**: 323–334. [Medline] [CrossRef]
10. Liontos, L. M., Dissanayake, D., Ohashi, P. S., Weiss, A., Dragone, L. L. and McGlade, C. J. 2011. The Src-like adaptor protein regulates GM-CSFR signaling and monocytic dendritic cell maturation. *J. Immunol.* **186**: 1923–1933. [Medline] [CrossRef]
11. Lundahl, J., Jacobson, S. H. and Paulsson, J. M. 2012. IL-8 from local subcutaneous wounds regulates CD11b activation. *Scand. J. Immunol.* **75**: 419–425. [Medline] [CrossRef]
12. Maurer, D., Fischer, G. F., Felzmann, T., Majdic, O., Gschwantler, E., Hinterberger, W., Wagner, A. and Knapp, W. 1991. Ratio of complement receptor over Fc-receptor III expression: a sensitive parameter to monitor granulocyte-monocyte colony-stimulating

factor effect on neutrophils. *Ann. Hematol.* **62**: 135–140. [Medline] [CrossRef]

13. McClure, B., Stomski, F., Lopez, A. and Woodcock, J. 2001. Perverted responses of the human granulocyte-macrophage colony-stimulating factor receptor in mouse cell lines due to cross-species beta-subunit association. *Blood* **98**: 3165–3168. [Medline] [CrossRef]
14. Min, L., Mohammad Isa, S. A., Shuai, W., Piang, C. B., Nih, F. W., Kotaka, M. and Ruedl, C. 2010. Granulocyte-macrophage colony-stimulating factor is the major CD8+ T cell-derived licensing factor for dendritic cell activation. *J. Immunol.* **184**: 4625–4629. [Medline] [CrossRef]
15. Neuman, E., Huleatt, J. W. and Jack, R. M. 1990. Granulocyte-macrophage colony-stimulating factor increases synthesis and expression of CR1 and CR3 by human peripheral blood neutrophils. *J. Immunol.* **145**: 3325–3332. [Medline]
16. Nothdurft, W., Selig, C., Fliedner, T. M., Hintz-Obertreis, P., Kreja, L., Krumwieh, D., Kurrle, R., Seiler, F. R. and Weinsheimer, W. 1992. Haematological effects of rhGM-CSF in dogs exposed to total-body irradiation with a dose of 2.4 Gy. *Int. J. Radiat. Biol.* **61**: 519–531. [Medline] [CrossRef]
17. Reddy, A., Sapp, M., Feldman, M., Subklewe, M. and Bhardwaj, N. 1997. A monocyte conditioned medium is more effective than defined cytokines in mediating the terminal maturation of human dendritic cells. *Blood* **90**: 3640–3646. [Medline]
18. Schuening, F. G., Storb, R., Goehle, S., Nash, R., Graham, T. C., Appelbaum, F. R., Hackman, R., Sandmaier, B. M. and Urdal, D. L. 1989. Stimulation of canine hematopoiesis by recombinant human granulocyte-macrophage colony-stimulating factor. *Exp. Hematol.* **17**: 889–894. [Medline]
19. Trapnell, B. C. and Whitsett, J. A. 2002. GM-CSF regulates pulmonary surfactant homeostasis and alveolar macrophage-mediated innate host-defense. *Annu. Rev. Physiol.* **64**: 775–802. [Medline] [CrossRef]
20. Uchida, K., Beck, D. C., Yamamoto, T., Berclaz, P.Y., Abe, S., Staudt, M. K., Carey, B. C., Filippi, M.D., Wert, S. E., Denson, L. A., Puchalski, J. T., Hauck, D. M. and Trapnell, B. C. 2007. GM-CSF autoantibodies and neutrophil dysfunction in pulmonary alveolar proteinosis. *N. Engl. J. Med.* **356**: 567–579. [Medline] [CrossRef]
21. Vreugdenhil, G., Preyers, F., Croockewit, S., Sauerwein, R., Swaak, A. J. and de Witte, T. 1992. Fever in neutropenic patients treated with GM-CSF representing enhanced host defence. *Lancet* **339**: 1118–1119. [Medline] [CrossRef]
22. Wang, Y-S., Chi, K-H., Liao, K-W., Liu, C-C., Cheng, C-L., Lin, Y-C., Cheng, C-H. and Chu, R-M. 2007. Characterization of canine monocyte-derived dendritic cells with phenotypic and functional differentiation. *Can. J. Vet. Res.* **71**: 165–174. [Medline]
23. Watanabe, S., Aoki, Y., Nishijima, I., Xu, M.J. and Arai, K. 2000. Analysis of signals and functions of the BA/F3 cells and transgenic mice colony-stimulating factor receptor in chimeric human granuloctye-macrophage. *J. Immunol.* **164**: 3635–3644. [Medline] [CrossRef]

Cytokine 68 (2014) 118–126

Contents lists available at ScienceDirect

Cytokine

journal homepage: www.journals.elsevier.com/cytokine

Low concentrations of recombinant granulocyte macrophage-colony stimulating factor derived from Chinese hamster ovary cells augments long-term bioactivity with delayed clearance *in vitro*

Atsushi Hashimoto [a], Takahiro Tanaka [a], Yuko Itoh [a], Akira Yamagata [b], Nobutaka Kitamura [c], Ryushi Tazawa [a], Kazuhide Nakagaki [d], Koh Nakata [a,*]

[a] *Bioscience Medical Research Center, Niigata University Medical and Dental Hospital, 1-754, Asahimachi-dori, Chuo-ku, Niigata 951-8510, Japan*
[b] *Towa Environment Science Co., Ltd. Prophoenix Division, 1-24-22 Nanko-kita, Suminoe, Osaka 559-0034, Japan*
[c] *Department of Medical Informatics, Niigata University Medical and Dental Hospital, 1-754, Asahimachi-dori, Chuo-ku, Niigata 951-8510, Japan*
[d] *Laboratory of Infectious Diseases and Immunology, College of Veterinary Medicine, Nippon Veterinary and Life Science University, 1-1-5, Sendagi, Bunkyo-ku, Tokyo 113-8602, Japan*

ARTICLE INFO

Article history:
Received 3 December 2013
Received in revised form 18 February 2014
Accepted 24 March 2014
Available online 9 May 2014

Keywords:
GM-CSF
TF-1 cells
CHO cells
Sialic acid
Oligosaccharide

ABSTRACT

To date, the biological activity of granulocyte macrophage-colony stimulating factor (GM-CSF) has been investigated by using mostly *Escherichia coli*- or yeast cell-derived recombinant human GM-CSF (erhGM-CSF and yrhGM-CSF, respectively). However, Chinese hamster ovary cell-derived recombinant human GM-CSF (crhGM-CSF), as well as natural human GM-CSF, is a distinct molecule that includes modifications by complicated oligosaccharide moieties. In the present study, we reevaluated the bioactivity of crhGM-CSF by comparing it with those of erhGM-CSF and yrhGM-CSF. The effect of short-term stimulation (0.5 h) on the activation of neutrophils/monocytes or peripheral blood mononuclear cells (PBMCs) by crhGM-CSF was lower than those with erhGM-CSF or yrhGM-CSF at low concentrations (under 60 pM). Intermediate-term stimulation (24 h) among the different rhGM-CSFs with respect to its effect on the activation of TF-1 cells, a GM-CSF-dependent cell line, or PBMCs was not significantly different. In contrast, the proliferation/survival of TF-1 cells or PBMCs after long-term stimulation (72–168 h) was higher at low concentrations of crhGM-CSF (15–30 pM) than that of cells treated with other GM-CSFs. The proportion of apoptotic TF-1 cells after incubation with crhGM-CSF for 72 h was lower than that of cells incubated with other rhGM-CSFs. These effects were attenuated by desialylation of crhGM-CSF. Clearance of crhGM-CSF but not desialylated-crhGM-CSF by both TF-1 cells and PBMCs was delayed compared with that of erhGM-CSF or yrhGM-CSF. These results suggest that sialylation of oligosaccharide moieties delayed the clearance of GM-CSF, thus eliciting increased long-term bioactivity *in vitro*.

1. Introduction

Granulocyte macrophage-colony stimulating factor (GM-CSF) is a hematopoietic growth factor that regulates the growth, differentiation, and maturation of myeloid precursor cells and promotes the function of mature neutrophils, eosinophils, and monocytes [1–4]. It elicits these diverse effects through interaction with a unique dodecameric receptor complex on cells, which consists of α and common β chains [5–7]. GM-CSF signaling induces phosphorylation of Janus kinase 2 (JAK2) and the common β chains, followed by activation of signal transducers and activators of transcription (STATs) [5,7,8]. Upon immune stimulation, it is produced by a variety of cell types, including T cells, macrophages, endothelial cells, and fibroblasts. Although GM-CSF is produced locally [3], it can

Abbreviations: ACN, acetonitrile; ANOVA, analysis of variance; CHO, Chinese hamster ovary; crhGM-CSF, CHO-derived recombinant human GM-CSF; erhGM-CSF, *Escherichia coli*-derived recombinant human GM-CSF; FCS, fetal calf serum; FITC, fluorescein isothiocyanate; GM-CSF, granulocyte macrophage-colony stimulating factor; JAK2, Janus kinase 2; MIP-1α, macrophage inflammatory protein; NaN_3, sodium azide; PBMCs, peripheral blood mononuclear cells; SDS-PAGE, sodium dodecyl sulfate–polyacrylamidegel electrophoresis; STAT5, signal transduction and activator of transcription; TFA, trifluoroacetic acid; TOF mass spectrometer, time-of-flight mass spectrometer; yrhGM-CSF, yeast cell-derived recombinant human GM-CSF.

* Corresponding author. Tel.: +81 25 227 0847.
E-mail addresses: noiredge2007@yahoo.co.jp (A. Hashimoto), belltatnk@gmail.com (T. Tanaka), y-itoh@med.niigata-u.ac.jp (Y. Itoh), yamagata@prophoenix.jp (A. Yamagata), nktmr@m12.alpha-net.ne.jp (N. Kitamura), ryushi@med.niigata-u.ac.jp (R. Tazawa), nakagaki@nvlu.ac.jp (K. Nakagaki), radical@med.niigata-u.ac.jp (K. Nakata).

http://dx.doi.org/10.1016/j.cyto.2014.03.009
1043-4666/

act in a paracrine fashion to recruit circulating neutrophils, monocytes, and lymphocytes to enhance their function in host defense [9,10]. GM-CSF is used clinically to prevent neutropenia and associated infections by promoting the proliferation of hematopoietic progenitor cells after chemotherapy, by promoting the differentiation of myeloid cells, and by enhancing the antibacterial activities of neutrophils and macrophages [10–14].

Natural human GM-CSF (hGM-CSF) has been purified from several sources, including medium conditioned with placenta cells or activated blood lymphocytes [15–19]. It is a glycoprotein that consists of 127 amino acid residues, with four cysteines involved in two disulfide bonds, forming a compact globular structure that comprises four α-helices joined by loops. It is found extracellularly as a homodimer [6,7] with two N-glycosylation sites at Asn27 and Asn37 and three O-glycosylation sites at Ser7, Ser9, and Thr10 [15]. The most heavily glycosylated hGM-CSF, with a molecular weight of 28–32 kDa, has two N-linked carbohydrate moieties, whereas the partially glycosylated hGM-CSF, with a molecular weight of 23–25 kDa, contains one N-linked carbohydrate moiety. A minimally glycosylated hGM-CSF with molecular weight of 16–18 kDa consists of only one O-linked carbohydrate [15,20].

Cells from various species can produce recombinant hGM-CSF (rhGM-CSF) [21,22]. However, only commercial preparations produced from *Escherichia coli* and *Saccharomyces cerevisiae* are available for clinical use. Commercial *E. coli*-derived recombinant hGM-CSF (erhGM-CSF), Molgramostim, is non-glycosylated, consists of 127 amino acid residues, has a molecular weight of 14.5 kDa, and is methylated at the N-terminal end [23]. Commercial *Saccharomyces*-derived recombinant hGM-CSF (yrhGM-CSF), Sargramostim, is a glycoprotein of 127 amino acids composed of three primary molecular species having molecular weights of 19.5, 16.8, and 15.5 kDa [23]. Its amino acid sequence differs from hGM-CSF by a substitution of leucine at position 23 [23]. On the other hand, rhGM-CSF derived from Chinese hamster ovary (CHO) cells (crhGM-CSF) has a molecular weight of 15–32 kDa with the same N-glycosylation and O-glycosylation sites as those of hGM-CSF, although the carbohydrate moieties added are probably different. Forno et al. demonstrated that the N-glycan terminal contains mono- and disialic acid residues, but has predominantly tri- or tetrasialic acid residues with and without N-acetyllactosamine repeat units. N-glycans contain more than 90% α-1,6-linked fucose at the proximal end [20].

The pattern of glycosylation on GM-CSF is known to affect its biological activity. Proliferation of a human monocytic leukemia cell line incubated with the heavily glycosylated hGM-CSF (28–32 kDa) was reduced six fold compared with proliferation after treatment with non-glycosylated erhGM-CSF, while neutrophil superoxide anion production was reduced by up to 10-fold. Partially glycosylated hGM-CSF (23–25 kDa) and minimally glycosylated hGM-CSF (16–18 kDa) have biological activity similar to that of erhGM-CSF. The binding capacity of these hGM-CSFs for the rhGM-CSF receptor on neutrophils decreases with increasing molecular weight [15]. Similarly, most studies on mammalian cell-derived, glycosylated GM-CSF (including crhGM-CSF) demonstrate that glycosylation of GM-CSF prolongs the *in vivo* half life by stabilizing the protein, but reduces its binding avidity to the GM-CSF receptor and decreases its biological activities such as colony-forming activity of bone marrow cells and neutrophil superoxide anion production [15,24].

In contrast to previous studies [15,24], we showed in the present study that glycosylated rhGM-CSF produced by CHO cells exhibited increased proliferation/survival of TF-1 cells, PBMCs and monocytes at low GM-CSF concentrations compared with that of erhGM-CSF and yrhGM-CSF *in vitro*. Desialylation of crhGM-CSF attenuated this effect, indicating that the sialyl residue is crucial for augmenting the long-term activity of GM-CSF. Moreover, we examined the mechanism of this effect by measuring the clearance of rhGM-CSF by cells.

2. Materials and methods

2.1. Material

2.1.1. Cells

TF-1, a GM-CSF-dependent cell line, was kindly provided by Kitamura et al. [22].

Peripheral blood mononuclear cells (PBMCs) and monocytes were isolated from the peripheral blood of healthy donors as described previously [8]. Written informed consent was obtained under protocols approved by the institutional review boards of the Niigata University Medical Dental Hospital.

2.1.2. rhGM-CSF

Molgramostim and Sargramostim were purchased from Amoytop Biotech Co., Ltd. (Xiamen, Fujian, PRC) and Genzyme Corporation (Cambridge, MA, USA), respectively. crhGM-CSF was kindly provided by JCR Pharmaceuticals Co., Ltd. (Ashiya, Hyogo, Japan).

2.1.3. Desialylation of crhGM-CSF

crhGM-CSF (1 mg/ml) was incubated with neuraminidase agarose from *Clostridium perfringens* (0.05 U/ml, Sigma–Aldrich, MO, USA) in 100 mM sodium acetate buffer with $CaCl_2$ (pH 5.0) for 60 min at 37 °C. After the agarose was removed, the solution was dialyzed against PBS overnight at 4 °C.

2.2. Mass spectrometry

Protein (10 μl) was mixed with 90 μl of 0.1% trifluoroacetic acid (TFA) and 0.5 μl of MB-HIC8 magnetic C8 beads (Bruker Daltonics, Hercules, MA, USA) in a PCR tube and then incubated for 5 min at room temperature. The tube was subsequently placed in a magnetic beads separator and the supernatant was removed by using a pipette. The magnetic beads were then washed three times with 100 μl of 0.1% TFA. The bound proteins were eluted from the magnetic beads by using 4.5 μl of 60% acetonitrile (ACN) in 0.1% TFA. Two microliters of the eluate was mixed with 1 μl of matrix solution (10 g/l sinapinic acid in 70% ACN, 0.1% TFA) and was spotted on a polished steel plate. The mass spectra were obtained on an Ultraflex TOF/TOF mass spectrometer (Bruker Daltonics, Hercules, MA, USA) operated in positive-ion linear mode.

2.3. Phosphorylated STAT5 detection assay

Heparinized fresh whole blood was incubated with 15, 30, 60, or 500 pM rhGM-CSF, for 30 min at 37 °C and fixed, and then red blood cells were lysed in Fix/Lyse buffer (BD Biosciences, Franklin Lakes, New Jersey, USA) for 20 min at 37 °C. White blood cells were collected by centrifugation and fixed in ice-cold methanol at −20 °C for 1 h. After centrifugation, the cells were resuspended in 3% FCS/0.01% NaN_3/PBS solution and incubated with Alexa Fluor 647-labeled anti-pSTAT5 (BD Biosciences, San Jose, CA, New Jersey, USA). Cells with phosphorylated STAT5 in granulocytes/monocytes detected by flow cytometry (Cell Analyzer, Sony, Tokyo, Japan).

2.4. Neutrophil CD11b stimulation index assay

The neutrophil CD11b assay was performed as described previously [25]. Aliquots of heparinized fresh whole blood were incubated with rhGM-CSF, and cell-surface CD11b levels were quantified by flow cytometry (Sony, Tokyo, Japan). The CD11b

stimulation index was calculated as the mean fluorescent intensity of stimulated neutrophils minus the mean fluorescent intensity of unstimulated neutrophils divided by the mean fluorescent intensity of unstimulated neutrophils and multiplied by 100.

2.5. Measurement of GM-CSF-induced MIP-1α in PBMCs

To evaluate GM-CSF-induced MIP-1α production in normal PBMCs, 1×10^6 cells were incubated with or without GM-CSF in macrophage-serum-free medium (GIBCO BRL, Palo Alto, CA, USA). MIP-1α levels in the supernatant were measured by ELISA (Quantikine, R&D Systems, Mincapolis, MN, USA) according to the manufacturer's instructions [26].

2.6. Cell proliferation/survival assay

TF-1 cells, PBMCs and monocytes (2×10^4 cells/well) were incubated with various concentrations of GM-CSF in macrophage serum free medium (GIBCO BRL, Palo Alto, CA, USA) for 3 and 7 days, respectively [27]. At the end of the incubation, 10 μl of 100 μl (5-[2,4-bis(sodiooxysulfonyl)phenyl-3-(2-methoxy-4-nitrophenyl)-2-(4-nitrophenyl)-2*H*-tetrazole-3-ium]) CCK-8, Doujindo, Kumamoto, Japan) was added to each well. Cells were further incubated at 37 °C under 5% CO_2 for 4 h, and formazan formation was measured as absorbance at 450 nm by using a microplate reader (Bio-Rad, CA, USA).

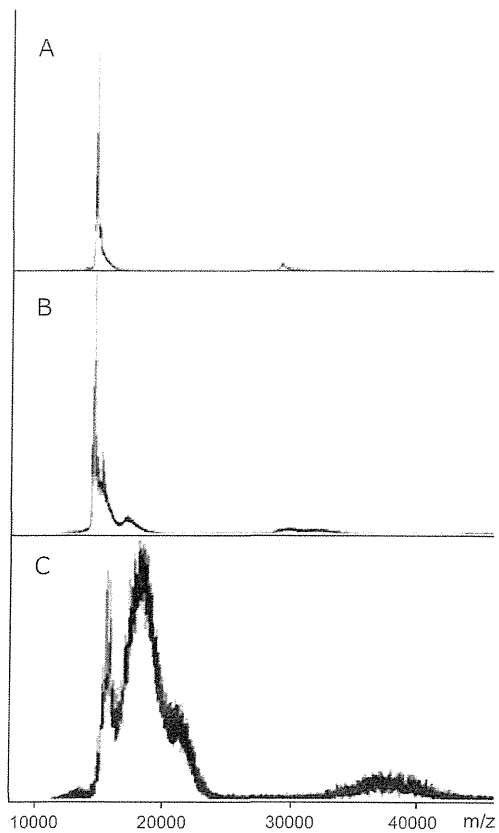

Fig. 1. Mass spectra of rhGM-CSFs. (A) *E. coli*-derived recombinant human GM-CSF. (B) Yeast-derived recombinant human GM-CSF. (C) CHO cell-derived recombinant human GM-CSF. The horizontal axis is the molecular weight (Da) and the vertical axis is the intensity.

2.7. Inhibition of TF-1 cell growth by antibodies

A cell proliferation/survival assay was performed in the presence or absence of 500 ng/ml goat anti-GM-CSF antibody (R&D Systems, Mincapolis, MN, USA), which was purified from the serum of a goat immunized with erhGM-CSF.

2.8. Morphology and cell-survival assay

TF-1 cells (1×10^5 cells) incubated with rhGM-CSF were cytocentrifuged at 200 rpm for 2 min by using a Cytospin (Thermo Scientific, Waltham, MA, USA) and were then stained with Diff-Quick (Sysmex, Hyogo, Japan). The sizes of five hundred cells were measured under a high magnification field by using a micrometer (MeCan Imaging, Saitama, Japan). The percentage of living cells was determined by flow cytometry (Sony, Tokyo, Japan) using staining with propidium iodide solution (Annexin-V-FLUOS Staining Kit, Roche, Basel, Switzerland) according to the manufacturer's instructions.

2.9. SDS–PAGE

rhGM-CSFs (6.5 ng) were subjected to SDS–PAGE under reducing conditions. The gel was stained by using gel stain solution (ORIOLE Fluorescent Gel Stain, Bio-Rad, CA, USA), and the banding pattern was visualized under an image analyzer (MiniLumi, Berthold Technologies, Bad Wildbad, Germany).

2.10. Detection of apoptosis

2.10.1. FITC-Annexin V preparation

TF-1 cells (1×10^6 cells) were stained with FITC-labeled anti-Annexin-V antibody (Annexin-V-FLUOS Staining Kit, Roche,

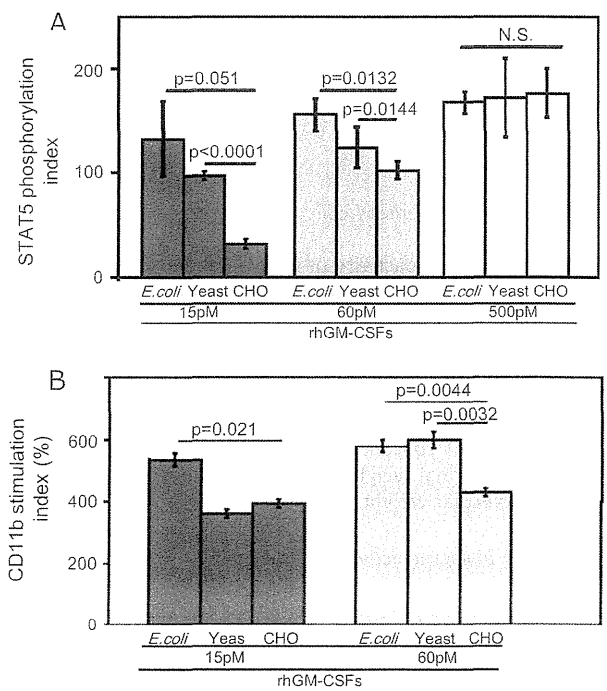

Fig. 2. Effect of short-term stimulation (0.5 h) by *E. coli*-, yeast-, and CHO cell-derived rhGM-CSF. The phosphorylation of STAT5 (A) and CD11b expression of neutrophils and monocytes (B). Whole blood cells were incubated for 0.5 h with 15, 60, or 500 pM of each rhGM-CSF for in (A) and 15 or 60 pM in (B). The vertical axis is STAT5 phosphorylation index (A) and CD11b stimulation index (B) is defined as described in Section 2.

Basel, Switzerland) for 15 min at 4 °C, and the stained cells were detected by flow cytometry (Sony, Tokyo, Japan). FITC-labeled mouse IgG isotype was used as the control.

2.10.2. DNA fragmentation assay

TF-1 cells (2×10^5 cells/ml) were incubated with 15 pM of rhGM-CSF for 3 days [27].

At the end of the incubation, DNA was extracted from TF-1 cells by using a QIAamp DNA Mini Kit (QIAGEN, Valencia, CA, USA). DNA (3.5 μg) was loaded on 1% agarose gel and electrophoresed for 25 min at 100 V (constant voltage). After the gel was stained with ethidium bromide solution (10 mg/ml, Nippon Gene, Tokyo, Japan), the banding pattern was visualized under an image analyzer (Mini-Lumi, Berthold Technologies, Bad Wildbad, Germany).

2.11. GM-CSF clearance assay

GM-CSF clearance assay was performed as described previously [8]. To assess receptor-mediated binding and uptake of exogenous GM-CSF, 1×10^6 PBMCs or 4×10^5 TF-1 cells per well in a 24-well culture plate were incubated in RPMI 1640 (GIBCO BRL, Palo Alto, CA, USA) containing 10% FCS (Nichirei, Bioscience Inc, Tokyo, Japan) 100 mg/ml streptomycin and 100 U/ml penicillin under 5% CO_2 at 37 °C. rhGM-CSF was added at concentrations of 5 and 15 pM to PBMCs and TF-1 cells, respectively. The concentration of rhGM-CSF in the supernatant of each well was then measured at 5, 10, 24, and 48 h by ELISA.

2.12. Statistical analysis

Numerical data were evaluated for normal distribution by using Shapiro–Wilk tests. Parametric data are presented as means (±SE). Parametric data were analyzed by using one-way factorial ANOVA measurements. Multiple comparisons were performed through a Bonferroni-adjusted *t*-test, with non-significance set at $p > 0.05$. All tests were two-sided and *p* values <0.05 were considered statistically significant. Data were analyzed by using JMP (10.0.0) software (SAS, Cary, NC, USA).

3. Results

3.1. Molecular weight of rhGM-CSF

In this study, the bioactivity of rhGM-CSF derived from *E. coli*, yeast, and CHO cells was evaluated and compared. The mass spectrum of each GM-CSF shows distinct characteristic peaks: a single peak at 14.5 kDa for erhGM-CSF; peaks at 14.2, 14.4, and 15.0 kDa for yrhGM-CSF corresponding to a mean molecular weight of 14.7 kDa; and a number of peaks ranging from 16–28 kDa for crhGM-CSF corresponding to mean molecular weight of 19.0 kDa (Fig. 1A). The molar concentration of each rhGM-CSF was calculated from the original weight and volume, and then dividing by each mean molecular weight.

3.2. Short-term biological activity of rhGM-CSF

To compare the short-term bioactivity of the three rhGM-CSFs, we first evaluated the phosphorylation of STAT5 in monocytes and neutrophils stimulated for 0.5 h with the rhGM-CSFs. At both 15 and 60 pM rhGM-CSF, the percentage of pSTAT5-positive cells was significantly lower in crhGM-CSF-treated cells than in erhGM-CSF- or yrhGM-CSF-treated cells; whereas at 500 pM, this percentage was similar among the three rhGM-CSFs (Fig. 2A). Maximal values of CD11b stimulation indices at 60 pM of rhGM-CSF were 425 ± 15%, 576 ± 27%, and 625 ± 33%, for crhGM-CSF, erhGM-CSF, and yrhGM-CSF, respectively (Fig. 2B). These results indicate that the short-term effect of stimulation with crhGM-CSF was smaller than that with erhGM-CSF and yrhGM-CSF.

3.3. Intermediate-term biological activity of rhGM-CSF

When TF-1 cells were incubated with 30–120 pM rhGM-CSF for 24 h, the proliferation/survival was similar after treatment with crhGM-CSF, erhGM-CSF, and yrhGM-CSF (Fig. 3A). Likewise, MIP-1α production in PBMCs was not different among the three rhGM-CSFs at both 15 and 500 pM (Fig. 3B).

3.4. Long-term biological activity of rhGM-CSF

We then investigated the long-term biological effect of GM-CSF on TF-1 cells, monocytes, and PBMCs incubated for 72, 168, and 168 h, respectively. The effect on the proliferation/survival rate of TF-1 cells was significantly greater in cells incubated with 15 pM crhGM-CSF than that on cells incubated with the same concentration of erhGM-CSF or yrhGM-CSF. However, the effects were equivalent among the three rhGM-CSFs at 60 pM. The ED_{50} of each rhGM-CSF was 21 and 24 pM for erhGM-CSF and yrhGM-CSF, respectively, whereas it was 3.9 pM for crhGM-CSF (Fig. 4A). When monocytes were incubated with the GM-CSFs, the proliferation/survival rate was higher at 4 pM crhGM-CSF than that of cells incubated with the same concentration of other GM-CSFs. The ED_{50} was 10.7, 4.9, and 1.8 pM for erhGM-CSF, yrhGM-CSF, and crhGM-CSF, respectively (Fig. 4B). Similarly, the proliferation/survival rate of PBMCs was higher with 2–4 pM crhGM-CSF compared with that with other GM-CSFs (Fig. 4C). Proliferation/survival in the presence of goat anti-GM-CSF antibody was comparable, whereas the

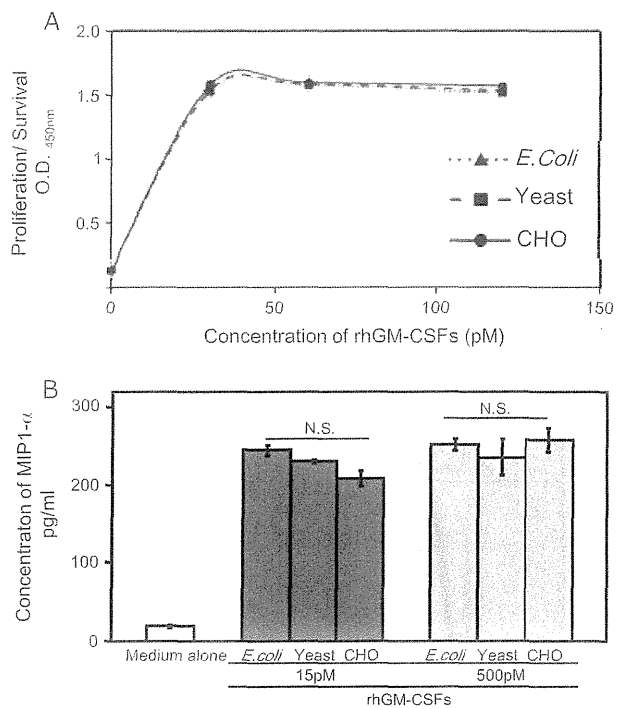

Fig. 3. Effect of intermediate-term stimulation (24 h) by rhGM-CSFs. (A) The proliferation/survival of TF-1 cells incubated for 24 h with various concentrations of rhGM-CSF derived from *E. coli* (▲), yeast (■), and CHO (●) was measured by MTT assay, as described in Section 2. The vertical axis indicates formazan formation expressed as the OD at 450 nm. (B) MIP-1α production of PBMCs incubated for 24 h with 0, 15, or 500 pM of *E. coli*, yeast-, and CHO-derived rhGM-CSF was measured by ELISA as described in Section 2.

inhibitory effect of the antibody was highest in crhGM-CSF. These data suggested that the effect of crhGM-CSF on the proliferation/survival of TF-1 cells was not due to oligosaccharide moieties but rather due to the GM-CSF peptide (Fig. 4D). After 3-day incubation with 30 pM erhGM-CSF, yrhGM-CSF, or crhGM-CSF, the number of viable TF-1 cells increased by multiples of 1.95 ± 0.5, 2.0 ± 0.7, and 6.45 ± 0.25, respectively, compared with the number of viable cells before incubation (Fig. 4E). The size histogram of TF-1 cells incubated with crhGM-CSF displays a bimodal pattern with a mean value of 24.09 μm, which is larger than that of erhGM-CSF-treated cells (22.09 μm) and yrhGM-CSF-treated cells (22.0 μm) (Fig. 4F). The viability of crhGM-CSF-stimulated TF-1 cells was significantly higher than that of TF-1 cells stimulated with other rhGM-CSFs. These results demonstrate that low concentrations of crhGM-CSF not only promote proliferation/survival but also stimulate the growth of these cells more efficiently than do erhGM-CSF and yrhGM-CSF, and that the long-term effect of rhGM-CSF differs from the short- and intermediate-term outcomes. The long-term effects of erhGM-CSF and yrhGM-CSF for each condition were similar.

3.5. Modified bioactivity of crhGM-CSF after treatment with sialidase

To investigate the effect of sialyl residues located at the distal end of the oligosaccharide moieties [20] on cell proliferation/survival, we studied sialidase-treated crhGM-CSF. After treatment, mass spectrometry revealed a drastic reduction in the intensity of peaks corresponding to mono-, di-, tri-, and tetra-sialyl carbohydrates (Fig. 5A). This is also consistent with the banding pattern

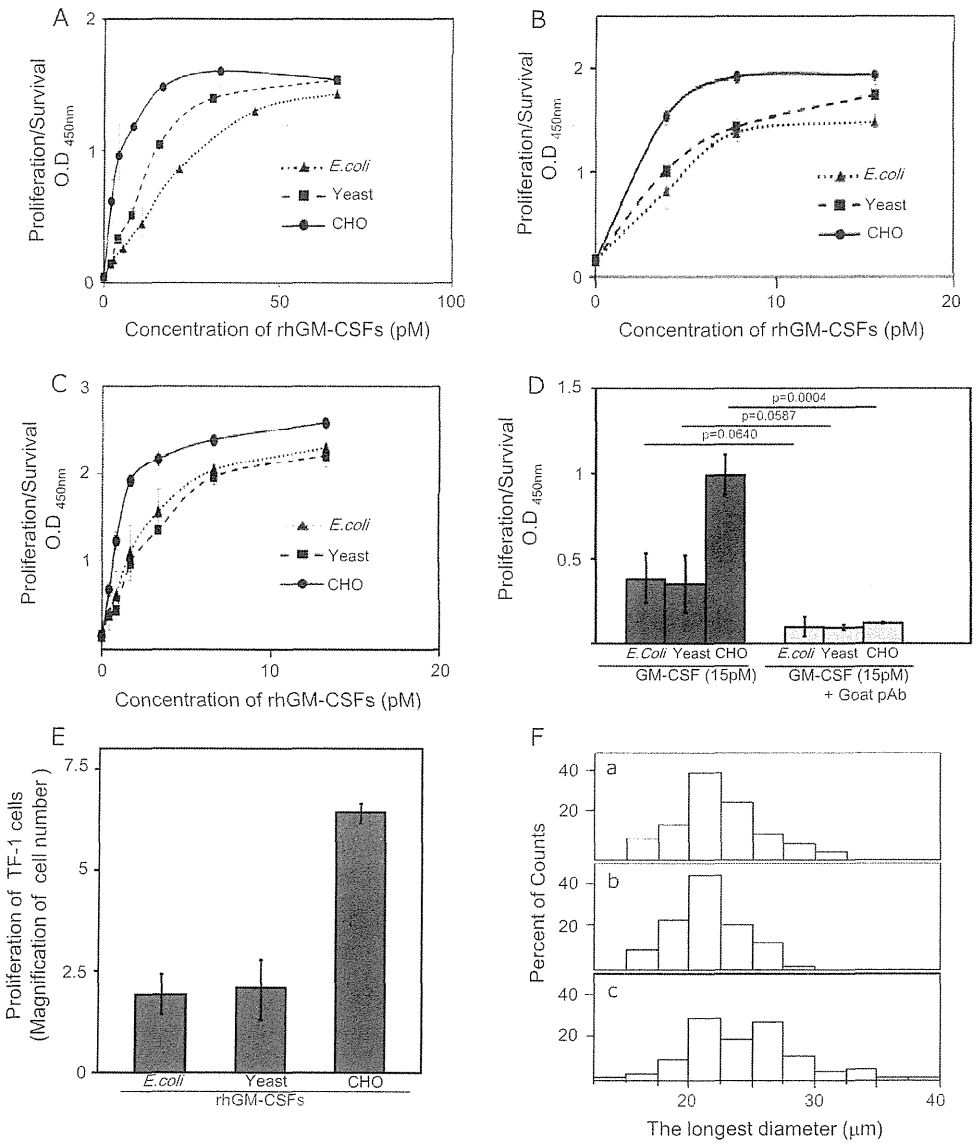

Fig. 4. Effect of long-term stimulation with various concentrations of rhGM-CSFs on the proliferation/survival of TF-1 cells, monocytes, and PBMCs. (A) Proliferation/survival of TF-1 cells incubated for 72 h with various concentrations (0–60 pM) of rhGM-CSF derived from *E. coli* (▲), yeast (■), and CHO (●) was measured as described in Section 2. (B) Proliferation/survival of monocytes incubated for 168 h with various concentrations (0–15 pM) of rhGM-CSF derived from *E. coli* (▲), yeast (■), and CHO (●) was measured as described in Section 2. (C) Proliferation/survival of PBMCs incubated for 168 h with various concentrations (0–15 pM) of rhGM-CSF derived from *E. coli* (▲), yeast (■), and CHO (●) was measured as described in Section 2. (D) Effect of neutralizing goat anti-*E. coli*-derived GM-CSF antibody on the proliferation/survival of TF-1 cells incubated with 15 pM rhGM-CSFs. The vertical axis is the proliferation/survival of TF-1 cells (OD at 450 nm). (E) Magnification of proliferation was measured by enumerating viable TF-1 cells under a phase contrast microscopy before and after 72 h incubation with 30 pM rhGM-CSFs. (F) Size distribution of TF-1 cells incubated with 15 pM rhGM-CSFs for 72 h. The horizontal axis is the largest diameter of cells and the vertical axis is the number of cells.

obtained by SDS–PAGE, in which several bands characteristic for crhGM-CSF are absent or weaker (Fig. 5B). Desialylation of crhGM-CSF markedly reduced the proliferation/survival rates to levels observed with erhGM-CSF- or yrhGM-CSF-treated cells (Fig. 5C). These results suggest that the up-regulated proliferation/survival induced by crhGM-CSF is likely due to its sialyl residues.

3.6. The effect of GM-CSF on apoptosis of TF-1 cells

The effect of GM-CSF on the apoptosis of TF-1 cells was evaluated by Annexin V expression with flow cytometry. When TF-1 cells were incubated with 30 pM crhGM-CSF for 3 days, 8.8% of the cells were apoptotic. In contrast, 17.0%, 21.4%, and 15.9% of cells were apoptotic upon incubation with erhGM-CSF, yrhGM-CSF, and sialidase-treated crhGM-CSF, respectively (Fig. 6A). TF-1 cells incubated with crhGM-CSF had fewer vacuolated nuclei and coagulated chromatin than those of cells incubated with other GM-CSFs (Fig. 6B). TF-1 cell apoptosis was also confirmed by DNA ladder formation via agarose gel electrophoresis (Fig. 6C). These results suggested that apoptotic TF-1 cells were less frequently observed in the presence of low concentration of crhGM-CSF than erhGM-CSF, yrhGM-CSF and sialidase-treated crh GM-CSF as TF-1 cells are GM-CSF dependent cell line. It is plausible that GM-CSF bioactivity is likely to remain in culture supernatant of the cells incubated with crhGM-CSF compared with other rhGM-CSFs.

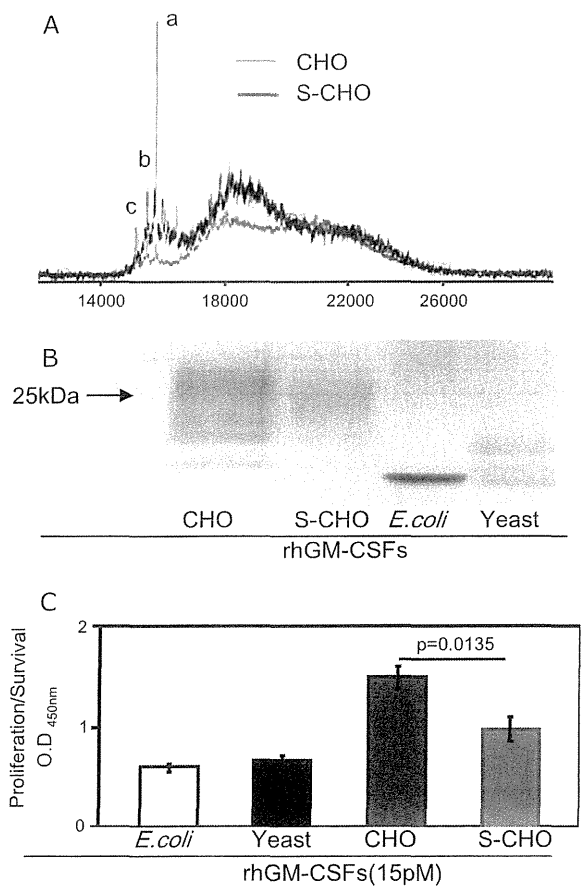

Fig. 5. Sialidase treatment of CHO-cell-derived rhGM-CSF and its biological activity. (A) Mass spectra of CHO cell-derived rhGM-CSF before (blue line) and after (red line) treatment with sialidase. (B) SDS–PAGE appearance of CHO cell-derived GM-CSF, CHO cell-derived GM-CSF after sialidase treatment, *E. coli*-derived GM-CSF, and yeast-derived GM-CSF. (C) The effect of sialidase treatment on the proliferation/survival of TF-1 cells after 72 h incubation with *E. coli*-, yeast-, CHO cells-derived rhGM-CSF or CHO cells-derived rhGM-CSF after sialidase treatment.

3.7. Clearance of rhGM-CSF by TF-1 cells and PBMCs

The clearance of crhGM-CSF by TF-1 cells and PBMCs was delayed compared with that of other GM-CSFs. After 24 and 48 h clearance assays, 13% and 9.5% of the initial crhGM-CSF concentration remained in the culture supernatant of PBMCs, whereas only 4.5% and 1.1% of erhGM-CSF, and 3.1%, 1% of yrhGM-CSF and 5.6% and 2.7% of sialidase-treated crhGM-CSF remained, respectively (Fig. 7A). On the other hand, after 24 and 48 h clearance assays, 7.5% and 3% of the initial crhGM-CSF concentration remained in the culture supernatant of TF-1 cells, whereas only 1.3% and 1.1% of erhGM-CSF, 1.1% and 1.0% of yrhGM-CSF and 2.9% and 2.7% of sialidase-treated crhGM-CSF remained, respectively (Fig. 7B). After 48 h incubation with erhGM-CSF, yrhGM-CSF, and sialidase treated crhGM-CSF, 15 pM of the same rhGM-CSF was except for crhGM-CSF added into each well. As shown in Fig. 7C, addition of each rhGM-CSF improved the proliferation/survival of TF-1 cells in the next 24 h reaching a similar level of those incubated with original 15 pM of crhGM-CSF for three days. Taken together with the data of proliferation/survival assay, it is likely that delayed clearance crhGM-CSF might prolong its biological activity *in vitro* (Fig. 7C).

4. Discussion

A number of studies have reported the expression of human GM-CSF by using natural or recombinant cells. These studies revealed that mammalian cells secrete GM-CSF proteins with variable molecular masses [20]. It has also been shown that its properties such as pharmacokinetics, binding affinity to the GM-CSF receptor, bioactivity, and immunogenicity are affected by glycosylation. In the present study, we demonstrated that compared with erhGM-CSF or yrhGM-CSF, crhGM-CSF promoted more efficiently the proliferation/survival of TF-1 cells, especially at low concentrations. In contrast to the results of the present study, natural hGM-CSF is thought to have lower biological activity with increasing glycosylation [15,24]. The pattern of glycosylation on GM-CSF has been found to affect its specific biological activity. Non-human expression systems such as yeast-, CHO cell-, or COS cell-derived rhGM-CSFs have distinct carbohydrate moieties and show different biological activities [18,28]. The half-life of hGM-CSF injected into rats decreases upon deglycosylation, indicating that the carbohydrate moieties influence the clearance, increase the stability, or alter the distribution of hGM-CSF. The carbohydrate structure of hematopoietic growth factors may therefore be important in determining their effective half-life *in vivo*. In this regard, we confirmed that *in vitro* GM-CSF clearance was also affected largely by the carbohydrate moieties of GM-CSF, especially its sialyl residues at the distal end of the oligosaccharide moieties.

The significance of the glycosylation of hematopoietic growth factors has been investigated previously. First, it is important for the secretion of glycoproteins. Erythropoietin secretion is prevented by site-directed mutagenesis of the N- or O-linked glycosylation sites [29–31]. As tunicamycin does not interfere with secretion of hGM-CSF, the N-linked carbohydrate is not crucial for this process [32]. Second, the N-linked carbohydrate influences the biological activity and receptor binding of other glycoprotein hormones and cytokines [29,33]. The *in vitro* activity of erythropoietin requires oligosaccharide moieties, but N-linked carbohydrates markedly reduce the *in vitro* activity of calcitonin. Glycosylation of luteinizing hormone is required for signal transduction, although

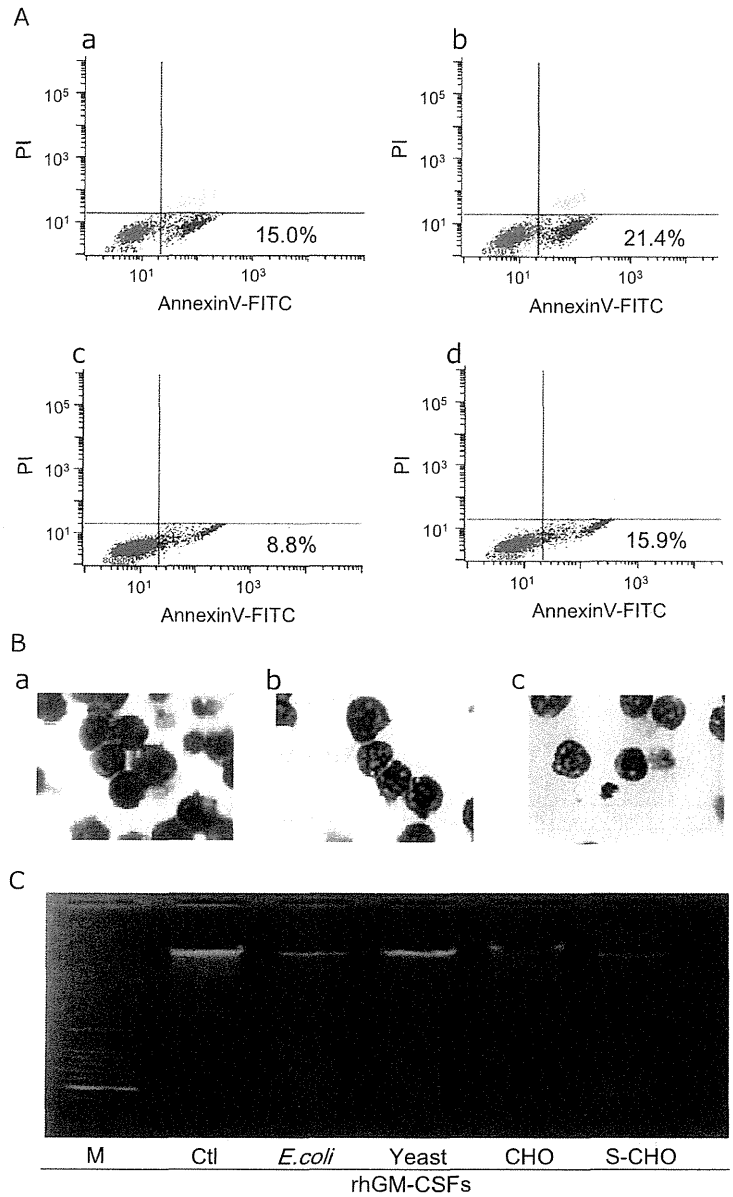

Fig. 6. Apoptosis of TF-1 cells incubated with 30 pM rhGM-CSFs for 72 h. (A) Flow cytometry results for apoptotic TF-1 cells incubated with rhGM-CSF derived from *E. coli* (a), yeast (b), CHO cells (c), or sialidase-treated CHO cells (d). The horizontal axis is the fluorescence intensity of Annexin V-FITC and the vertical axis is the fluorescence intensity of propidium iodide. (B) Morphology of TF-1 cells incubated with GM-CSF derived from CHO cells (a), yeast (b), and *E. coli* (c) at high magnification (1000×). Cells were cytocentrifuged and stained with Diff-Quick stain. (C) Agarose gel electropherogram of DNA extracted from TF-1 cells incubated with *E. coli*-, yeast-, CHO cells-derived rhGM-CSF or CHO cells-derived rhGM-CSF after sialidase treatment.

deglycosylated luteinizing hormone has higher receptor binding affinity [33]. Similarly, deglycosylation of hGM-CSF increases the receptor binding affinity [15]. However, in contrast to hGM-CSF, the most active forms are heavily glycosylated in luteinizing hormone [32].

Sialyl residues on carbohydrates in crhGM-CSF are considered crucial to the upregulation of the proliferation/survival of TF-1 cells because desialylation remarkably reduces this effect. Various sialylated forms of GM-CSF are produced in various tissues of mice and confer different physicochemical characteristics to murine GM-CSF [34]. Molecular weights of GM-CSF purified from various organs range from 37 to 200 kDa [32]; thus, it is possible that the bioactivity of GM-CSF produced in different tissues is regulated by the degree of sialylation. Since sialyl residues at the distal end of oligosaccharides can affect the specific activity of hGM-CSF as well as its isoelectric points and affinities to the GM-CSF receptor, sialylation may alter the activity of hGM-CSF in a tissue-specific manner. The aforementioned studies are clinically important because therapy using hGM-CSF has been associated with side effects, which may relate to its activities as a mediator of inflammation rather than to its function as a growth factor [15]. If different glycosylation patterns allow hGM-CSF activity to be regulated, manipulation of the carbohydrate moieties may enable reduction of the inflammatory mediator effects of hGM-CSF without affecting the stimulation of myeloid cell production.

GM-CSF exerts its biological activities by binding to specific high-affinity cell-surface receptors. After binding, the ligand/receptor complex is rapidly internalized in most hematopoietic cells [35,36]. It is not fully known whether the turnover time of this internalization differs between different rhGM-CSFs. It is possible

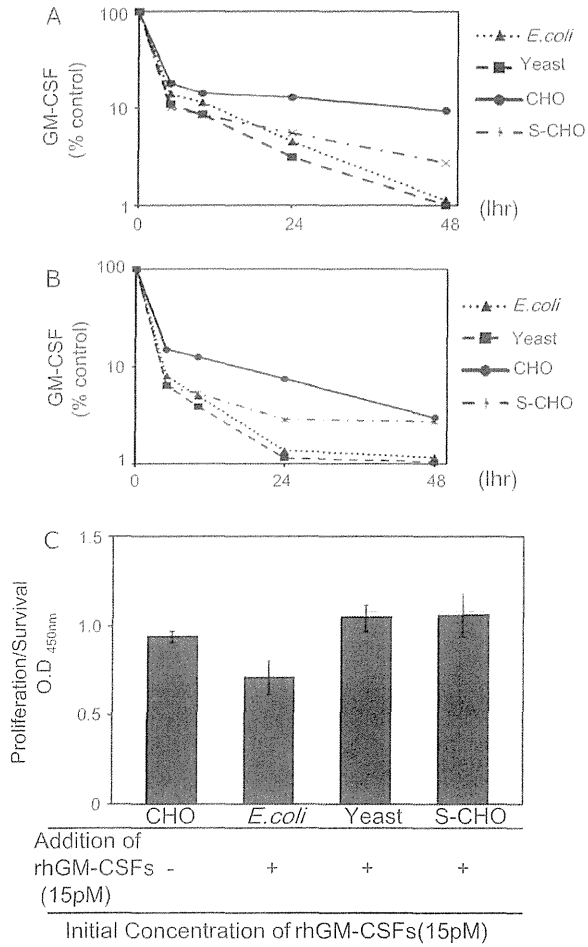

Fig. 7. GM-CSF clearance assay of TF-1 cells and peripheral blood mononuclear cells. (A) Peripheral blood mononuclear cells were incubated for 0–48 h with each 15 pM of *E. coli*-, yeast-, CHO cells-derived rhGM-CSF or CHO cells-derived rhGM-CSF after sialidase treatment. (B) TF-1 cells were incubated for 0–48 h with each 15 pM of *E. coli*-, yeast-, CHO cells-derived rhGM-CSF or CHO cells-derived rhGM-CSF after sialidase treatment. The horizontal axis is the time after the start of incubation. The vertical access is percent each rhGM-CSF concentration per initial concentration at each time point in the culture supernatant. (C) After 48 h incubation with *E. coli*-, yeast-, CHO cells-derived rhGM-CSF or CHO cells-derived rhGM-CSF after sialidase treatment, 15 pM of the same rhGM-CSF was added into each well. The vertical axis is the proliferation/survival of TF-1 cells (OD at 450 nm).

that the oligosaccharide sialyl residue of crhGM-CSF can attenuate its binding to the low-affinity rhGM-CSF receptor α and/or associate with the rhGM-CSF β chain, resulting in downregulation of signal transduction and delayed clearance of the molecule [15]. The present study revealed that stimulation with low concentrations of crhGM-CSF augmented STAT5 phosphorylation less effectively than did low concentrations of erhGM-CSF and yrhGM-CSF. The sialyl residue may prolong the turnover cycle (known to be 40 s for erhGM-CSF) and thus maintain rhGM-CSF bioactivity for a longer period [35]. In the future, it is necessary to determine whether the sialyl residues of GM-CSF attenuate its binding to low-affinity receptors on hematopoietic cells or delay the process of its internalization into cells.

5. Conclusion

We have demonstrated for the first time that sialylated oligosaccharide moieties prolong the proliferation/survival of rhGM-CSF *in vitro*. Further studies are warranted to determine the correlation of the oligosaccharide structure of crhGM-CSF with both signal transduction and internalization.

Authorship

A. Hashimoto and K. Nakata wrote the manuscript and designed the project.

A. Hashimoto performed experiments. Y. Ito and A. Yamagata assisted technical issues. T. Tanaka and N. Kitamurta contributed to the statistical analysis of data. R. Tazawa participated in preparation of materials. K. Nakagaki provided variable information for methods. All authors read and approved the final manuscript.

Disclosure

The authors declare that they have no competing interests.

Acknowledgments

The authors thank JCR Pharmaceuticals Co., Ltd. for providing valuable information on recombinant Chinese hamster ovary cell derived GM-CSF. We also thank Takuji Suzuki, Kiyoko Akagawa, Tomoyuki Kawase, Takahito Nei, Takuro Sakagami and Kanji Uchida for valuable discussions and critical review of this manuscript. We appreciate Maiko Higuchi for technical help and Marie Mori for assistance of manuscript submission.

References

[1] Atkinson YH, Lopez AF, Marasco WA, Lucas CM, Wong GG, Burns GF, et al. Recombinant human granulocyte-macrophage colony-stimulating factor (rH GM-CSF) regulates f Met-Leu-Phe receptors on human neutrophils. Immunology 1988;64:519–25.
[2] Burgess AW, Begley CG, Johnson GR, Lopez AF, Williamson DJ, Mermod JJ, et al. Purification and properties of bacterially synthesized human granulocyte-macrophage colony stimulating factor. Blood 1987;69:43–51.
[3] Metcalf D. Hematopoietic cytokines. Blood 2008;111:485–91.
[4] Esnault S, Malter JS. GM-CSF regulation in eosinophils. Arch Immunol Ther Exp (Warsz) 2002;50:121–30.
[5] Guthridge MA, Stomski FC, Thomas D, Woodcock JM, Bagley CJ, Berndt MC, et al. Mechanism of activation of the GM-CSF, IL-3, and IL-5 family of receptors. Stem Cells 1998;16:301–13.
[6] Hansen G, Hercus TR, McClure BJ, Stomski FC, Dottore M, Powell J, et al. The structure of the GM-CSF receptor complex reveals a distinct mode of cytokine receptor activation. Cell 2008;134:496–507.
[7] Martinez-Moczygemba M, Huston DP. Biology of common beta receptor-signaling cytokines: IL-3, IL-5, and GM-CSF. J Allergy Clin Immunol 2003;112:653–65 [quiz 66].
[8] Tanaka T, Motoi N, Tsuchihashi Y, Tazawa R, Kaneko C, Nei T, et al. Adult-onset hereditary pulmonary alveolar proteinosis caused by a single-base deletion in CSF2RB. J Med Genet 2011;48:205–9.
[9] Hercus TR, Thomas D, Guthridge MA, Ekert PG, King-Scott J, Parker MW, et al. The granulocyte-macrophage colony-stimulating factor receptor: linking its structure to cell signaling and its role in disease. Blood 2009;114:1289–98.
[10] Trapnell BC, Whitsett JA. Gm-CSF regulates pulmonary surfactant homeostasis and alveolar macrophage-mediated innate host defense. Annu Rev Physiol 2002;64:775–802.
[11] Huang FF, Barnes PF, Feng Y, Donis R, Chroneos ZC, Idell S, et al. GM-CSF in the lung protects against lethal influenza infection. Am J Respir Crit Care Med 2011;184:259–68.
[12] Weisbart RH, Golde DW, Clark SC, Wong GG, Gasson JC. Human granulocyte-macrophage colony-stimulating factor is a neutrophil activator. Nature 1985;314:361–3.
[13] Socinski MA, Cannistra SA, Sullivan R, Elias A, Antman K, Schnipper L, et al. Granulocyte-macrophage colony-stimulating factor induces the expression of the CD11b surface adhesion molecule on human granulocytes *in vivo*. Blood 1988;72:691–7.
[14] Shibata Y, Berclaz PY, Chroneos ZC, Yoshida M, Whitsett JA, Trapnell BC. GM-CSF regulates alveolar macrophage differentiation and innate immunity in the lung through PU.1. Immunity 2001;15:557–67.
[15] Cebon J, Nicola N, Ward M, Gardner I, Dempsey P, Layton J, et al. Granulocyte-macrophage colony stimulating factor from human lymphocytes. The effect of glycosylation on receptor binding and biological activity. J Biol Chem 1990;265:4483–91.
[16] Broudy VC, Kaushansky K, Segal GM, Harlan JM, Adamson JW. Tumor necrosis factor type alpha stimulates human endothelial cells to produce granulocyte/

macrophage colony-stimulating factor. Proc Natl Acad Sci USA 1986;83:7467–71.
[17] Fibbe WE, van Damme J, Billiau A, Voogt PJ, Duinkerken N, Kluck PM, et al. Interleukin-1 (22-K factor) induces release of granulocyte–macrophage colony-stimulating activity from human mononuclear phagocytes. Blood 1986;68:1316–21.
[18] Lee F, Yokota T, Otsuka T, Gemmell L, Larson N, Luh J, et al. Isolation of cDNA for a human granulocyte–macrophage colony-stimulating factor by functional expression in mammalian cells. Proc Natl Acad Sci USA 1985;82:4360–4.
[19] Gabrilove JL, Welte K, Harris P, Platzer E, Lu L, Levi E, et al. Pluripoietin alpha: a second human hematopoietic colony-stimulating factor produced by the human bladder carcinoma cell line 5637. Proc Natl Acad Sci USA 1986;83:2478–82.
[20] Forno G, Bollati Fogolin M, Oggero M, Kratje R, Etcheverrigaray M, Conradt HS, et al. N- and O-linked carbohydrates and glycosylation site occupancy in recombinant human granulocyte–macrophage colony-stimulating factor secreted by a Chinese hamster ovary cell line. Eur J Biochem 2004;271:907–19.
[21] Sieff CA. Hematopoietic growth factors. J Clin Invest 1987;79:1549–57.
[22] Kitamura T, Tange T, Terasawa T, Chiba S, Kuwaki T, Miyagawa K, et al. Establishment and characterization of a unique human cell line that proliferates dependently on GM-CSF, IL-3, or erythropoietin. J Cell Physiol 1989;140:323–34.
[23] Dorr RT. Clinical properties of yeast-derived versus *Escherichia coli*-derived granulocyte–macrophage colony-stimulating factor. Clin Ther 1993;15:19–29 [discussion 18].
[24] Moonen P, Mermod JJ, Ernst JF, Hirschi M, DeLamarter JF. Increased biological activity of deglycosylated recombinant human granulocyte/macrophage colony-stimulating factor produced by yeast or animal cells. Proc Natl Acad Sci USA 1987;84:4428–31.
[25] Uchida K, Nakata K, Suzuki T, Luisetti M, Watanabe M, Koch DE, et al. Granulocyte/macrophage-colony-stimulating factor autoantibodies and myeloid cell immune functions in healthy subjects. Blood 2009;113:2547–56.
[26] Rosen LB, Freeman AF, Yang LM, Jutivorakool K, Olivier KN, Angkasekwinai N, et al. Anti-GM-CSF autoantibodies in patients with cryptococcal meningitis. J Immunol 2013;190:3959–66.
[27] Uchida K, Beck DC, Yamamoto T, Berclaz PY, Abe S, Staudt MK, et al. GM-CSF autoantibodies and neutrophil dysfunction in pulmonary alveolar proteinosis. N Engl J Med 2007;356:567–79.
[28] Nicola NA, Metcalf D, Johnson GR, Burgess AW. Separation of functionally distinct human granulocyte–macrophage colony-stimulating factors. Blood 1979;54:614–27.
[29] Dube S, Fisher JW, Powell JS. Glycosylation at specific sites of erythropoietin is essential for biosynthesis, secretion, and biological function. J Biol Chem 1988;263:17516–21.
[30] Teh SH, Fong MY, Mohamed Z. Expression and analysis of the glycosylation properties of recombinant human erythropoietin expressed in *Pichia pastoris*. Genet Mol Biol 2011;34:464–70.
[31] Darling RJ, Kuchibhotla U, Glaesner W, Micanovic R, Witcher DR, Beals JM. Glycosylation of erythropoietin affects receptor binding kinetics: role of electrostatic interactions. Biochemistry 2002;41:14524–31.
[32] Jonathan Cebon, Burgess Antony W. Glycosylation of human granulocyte-macrophage colony stimulating factor alters receptor binding and biological activity. TIGG 1991;3(12).
[33] Sairam MR, Bhargavi GN. A role for glycosylation of the alpha subunit in transduction of biological signal in glycoprotein hormones. Science 1985;229:65–7.
[34] Walker F, Burgess AW. Specific binding of radioiodinated granulocyte-macrophage colony-stimulating factor to hemopoietic cells. Embo J 1985;4:933–9.
[35] Elliott MJ, Moss J, Dottore M, Park LS, Vadas MA, Lopez AF. Differential binding of IL-3 and GM-CSF to human monocytes. Growth Factors 1992;6:15–29.
[36] Walker F, Burgess AW. Internalisation and recycling of the granulocyte-macrophage colony-stimulating factor (GM-CSF) receptor on a murine myelomonocytic leukemia. J Cell Physiol 1987;130:255–61.

Am J Physiol Lung Cell Mol Physiol 308: L105–L117, 2015.
First published November 14, 2014; doi:10.1152/ajplung.00239.2014.

CALL FOR PAPERS *Bioengineering the Lung: Molecules, Materials, Matrix, Morphology, and Mechanics*

A mathematical model to predict protein wash out kinetics during whole-lung lavage in autoimmune pulmonary alveolar proteinosis

Keiichi Akasaka,[1] Takahiro Tanaka,[1] Takashi Maruyama,[2] Nobutaka Kitamura,[1] Atsushi Hashimoto,[1] Yuko Ito,[1] Hiroyoshi Watanabe,[3] Tomoshige Wakayama,[3] Takero Arai,[4] Masachika Hayashi,[5] Hiroshi Moriyama,[5] Kanji Uchida,[6] Shinya Ohkouchi,[7] Ryushi Tazawa,[1] Toshinori Takada,[8] Etsuro Yamaguchi,[9] Toshio Ichiwata,[10] Masaki Hirose,[11] Toru Arai,[11] Yoshikazu Inoue,[11] Hirosuke Kobayashi,[12] and Koh Nakata[1]

[1]*Bioscience Medical Research Center, Niigata University Medical and Dental Hospital, Niigata, Japan;* [2]*Disaster Prevention Research Institute, Kyoto University, Kyoto, Japan;* [3]*Department of Respiratory Medicine, Dokkyo Medical University Koshigaya Hospital, Saitama, Japan;* [4]*Department of Anesthesiology, Dokkyo Medical University Koshigaya Hospital, Saitama, Japan;* [5]*Division of Respiratory Medicine, Niigata University Medical and Dental Hospital, Niigata, Japan;* [6]*Department of Anesthesiology, Graduate School of Medicine, The University of Tokyo, Tokyo, Japan;* [7]*Department of Respiratory Medicine, Tohoku University Graduate school of Medicine, Miyagi, Japan;* [8]*Uonuma Institute of Community Medicine, Niigata University Medical and Dental Hospital, Niigata, Japan;* [9]*Department of Respiratory and Allergy Medicine, Aichi Medical University, Aichi, Japan;* [10]*Department of Pulmonary Medicine, Tokyo Medical University Hachioji Medical Center, Tokyo, Japan;* [11]*Clinical Research Center, NHO Kinki-Chuo Chest Medical Center, Osaka, Japan; and* [12]*Graduate School of Medical Sciences, Kitasato University, Kanagawa, Japan*

Submitted 4 September 2014; accepted in final form 10 November 2014

Akasaka K, Tanaka T, Maruyama T, Nobutaka Kitamura, Hashimoto A, Ito Y, Watanabe H, Wakayama T, Arai T, Hayashi M, Moriyama H, Uchida K, Ohkouchi S, Tazawa R, Takada T, Yamaguchi E, Ichiwata T, Hirose M, Arai T, Inoue Y, Kobayashi H, Nakata K. A mathematical model to predict protein wash out kinetics during whole-lung lavage in autoimmune pulmonary alveolar proteinosis. *Am J Physiol Lung Cell Mol Physiol* 308: L105–L117, 2015. First published November 14, 2014; doi:10.1152/ajplung.00239.2014.—Whole-lung lavage (WLL) remains the standard therapy for pulmonary alveolar proteinosis (PAP), a process in which accumulated surfactants are washed out of the lung with 0.5–2.0 l of saline aliquots for 10–30 wash cycles. The method has been established empirically. In contrast, the kinetics of protein transfer into the lavage fluid has not been fully evaluated either theoretically or practically. Seventeen lungs from patients with autoimmune PAP underwent WLL. We made accurate timetables for each stage of WLL, namely, instilling, retaining, draining, and preparing. Subsequently, we measured the volumes of both instilled saline and drained lavage fluid, as well as the concentrations of proteins in the drained lavage fluid. We also proposed a mathematical model of protein transfer into the lavage fluid in which time is a single variable as the protein moves in response to the simple diffusion. The measured concentrations of IgG, transferrin, albumin, and β_2-microglobulin closely matched the corresponding theoretical values calculated through differential equations. Coefficients for transfer of β_2-microglobulin from the blood to the lavage fluid were two orders of magnitude higher than those of IgG, transferrin, and albumin. Simulations using the mathematical model showed that the cumulative amount of eliminated protein was not affected by the duration of each cycle but dependent mostly on the total time of lavage and partially on the volume instilled. Although physicians have paid little attention to the transfer of substances from the lung to lavage fluid, WLL seems to be a procedure that follows a diffusion-based mathematical model.

pulmonary alveolar proteinosis; granulocyte/macrophage colony-stimulating factor autoantibody; whole-lung lavage; protein transfer rate

PULMONARY ALVEOLAR PROTEINOSIS (PAP) is a rare lung disorder in which surfactant-associated phospholipids and proteins abnormally accumulate within alveoli and terminal bronchioles, leading to impaired gas exchange and progressive respiratory failure (6, 33, 40). PAP is classified into three groups based on etiology: autoimmune PAP (aPAP), secondary PAP, and hereditary PAP (6, 17, 40). aPAP is caused by granulocyte/macrophage colony-stimulating factor (GM-CSF) autoantibodies, which prevent surfactant removal by alveolar macrophages (20, 41). aPAP is the most prevalent form of PAP, comprising 90% of all PAP cases (6, 17, 40). Currently, whole-lung lavage (WLL) remains the only standard therapy for aPAP (4, 7, 29). Although WLL improves PAP in about 85–95% of patients, around 15–66% of such patients may require multiple and repeated WLL therapy (1, 4, 37). Removal of the lipoproteinous material by WLL immediately improves both lung volume and ventilation/perfusion ratio, leading to a marked increase in arterial oxygen gas pressure (5, 29, 36). In contrast, the diffusion capacity recovers gradually and incompletely over a 6-mo period (36). In addition, WLL decreases the area of ground-glass opacities but not reticular opacities and inter-

Address for reprint requests and other correspondence: K. Nakata, Bioscience Medical Research Center, Niigata Univ. Medical and Dental Hospital, 1-754 Asahimachi-dori, Niigata 951-8520, Japan (e-mail: radical@med.niigata-u.ac.jp)

lobular septal thickening (24). These observations suggest that the efficacy of WLL is not attributable to simple exclusion of accumulated surfactants but rather attributable to the recovery of normal lung structure and function.

GM-CSF autoantibodies and various other proteins (with the exception of large molecules such as IgM) have been reported to transfer the air-blood barrier (2, 9, 39). Both IgG1/albumin and IgG2/albumin ratios of the serum and bronchoalveolar lavage fluid (BALF) are similar, indicating transfer of these proteins (28). IgG most probably migrates by epithelial transcytosis or by paracellular diffusion through the air-blood barrier (13). In the steady state, the air-blood barrier consists of endothelial cells, basement membrane, epithelial cells, and surfactant film (8, 15). Surfactant film reduces leakage of plasma proteins to a minimum (15). In a previous study, disruption of surface tension-lowering properties of surfactant protein B (SP-B) in conditional knockout mice led to constriction of alveolar capillaries that resulted in protein leaks, lung edema, and alterations in alveolar surface area (15). Although no report describes the disruption of air-blood barrier after lung lavage, it is plausible that WLL removes the surfactant film from the alveolar surface followed by leaking plasma proteins.

In the present study, the kinetics of transfer of proteins from the blood and the surfactant to the lavage fluid was examined by measuring their concentrations in aliquots of lavage fluid drained during WLL. For this purpose, we proposed a mathematical model that can account for the transfer of proteins from the blood and the surfactant to the lavage fluid. The transmission coefficients were optimized, and the temporal variations of protein concentrations were simulated. Finally, the proposed model was evaluated by comparison with the measured data. Moreover, we showed the limitations of the present model.

Glossary

A_b	The effective surface area from the blood
A_s	The effective surface area from the surfactant
K_b	The transmission coefficient from the blood
K_s	The transmission coefficient from the surfactant
m_b	The masses of protein in the blood
$m_{in\text{-}out}$	The masses of protein in instilling saline and draining lavage fluid; actually, no protein exists in instilling saline
m_l	The masses of protein in the lavage fluid
m_{out}	The protein mass of drainage
m_s	The masses of protein in the surfactant
R_{cl}	The absorption rate of fluid into the circulation
S_A	The alveolar surface area
V_A	The alveolar volume
V_b	The volume of blood
V_{in}	The fluid volume of instilled saline
V_l	The volume of lavage
$V_{l\text{-}b}$	The fluid volume absorbed into the circulation
V_{out}	The fluid volume of drainage
V_s	The volume of surfactant

MATERIALS AND METHODS

Participants

Nine patients were enrolled in five hospitals in Japan. These hospitals included Tohoku University Hospital, Tokyo Medical University Hachioji Hospital, Aichi Medical University Hospital, Dokkyo Medical University Koshigaya Hospital, and Niigata University Medical and Dental Hospital. Diagnosis of aPAP was performed on the basis of cytological analysis of BALF, pulmonary histopathological findings, or both with high-resolution computed tomography appearance (40). All cases were confirmed to have elevated serum GM-CSF autoantibody levels (21, 41). The institutional review board of each hospital approved the study, and all subjects provided written informed consent. The study protocol was designed according to The Ethical Guideline of Clinical Research by The Japanese Ministry of Health, Labour, and Welfare in 2008.

Data of arterial blood gas analyses and serum markers were collected within 3 days, and pulmonary function tests were within 2 wk prior to WLL.

Procedure of WLL

Seventeen lungs from nine patients with aPAP underwent WLL. We allowed each participating hospital to conduct WLL in accordance with their own procedures. Generally, after administration of general anesthesia, patients were intubated with a double-lumen endotracheal tube to isolate the lungs, after which mechanical ventilation was initiated. After ventilation of the bilateral lungs with 100% oxygen for 5–15 min, saline was instilled into the lavage lung while ventilation of the other lung with 100% oxygen was continued. The instilled saline was then retained for a few minutes and then discharged by gravity into a container until a decrease in outflow was observed. These procedures were then repeated. In each lavage cycle, we prepared a timetable to record the exact time (to the second) of the start of instilling saline, the start of retaining, and the start and end of lavage fluid draining. We measured the volume of drained lavage fluid and used a 10-ml aliquot for further analyses. All samples were stored at −80°C until use.

Measurement of Substance Concentration

The serum and BALF concentration of IgG, GM-CSF autoantibody, transferrin, albumin, β_2-microglobulin, urea, gastrin, and SP-D were measured; IgG were quantified by an ELISA system using Human IgG ELISA Quantitation Set (Bethyl Laboratories, Montgomery, AL) according to the manufacturer's instructions. GM-CSF autoantibody concentrations were measured by an ELISA system as described previously (17). β_2-Microglobulin, gastrin, urea, and SP-D concentrations were measured by latex agglutination immunoassay (LA; LZ test Eiken β_2-M-II; Eiken, Tokyo Japan), radioimmunoassay (gastrin RIA kit II; Fujirebio, Tokyo, Japan), urease-indophenol method (urea nitrogen test; Wako, Tokyo, Japan), and enzyme immunoassay (SP-D kit Yamasa EIA II; Yamasa, Tokyo, Japan), respectively. Serum transferrin and albumin concentrations were measured by turbidimetric immunoassay (TIA; N-Assay TIA Tf-H Nittobo; Nittobo, Tokyo, Japan) and bromocresol purple dye-binding assay (PureAuto A ALB; Kainos, Toyko, Japan), respectively, and those in the BALF were analyzed by LA (N-Assay LA Micro Tf Nittobo) and TIA (AutoWako Microalbumin). These serum samples were collected just before the beginning of WLL.

A Mathematical Kinetic Model to Estimate the Concentration of Proteins in the Lavage Fluid

We postulated that proteins both in the accumulated surfactant material and in the pulmonary capillaries transfer into the lavage fluid. Under such circumstances, the rate of protein transfer to the lavage fluid is assumed to be as follows:

$$\frac{dm_l}{dt} = \frac{dm_s}{dt} + \frac{dm_b}{dt} + \frac{dm_{in-out}}{dt} \quad (1)$$

where the first term in the right-hand side is the transfer rate from surfactant, the second term is the transfer rate from blood, and the

third term is the rate of instilling and drainage. The transfer rate from surfactant dm_s/dt and the transfer rate from blood dm_b/dt are modeled by analogy to the heat transmission model as

$$\frac{dm_s}{dt} = K_S \cdot A_S\left(\frac{m_s}{V_s} - \frac{m_l}{V_l}\right) \quad (2)$$

$$\frac{dm_b}{dt} = K_b \cdot A_b\left(\frac{m_b}{V_b} - \frac{m_l}{V_l}\right) \quad (3)$$

where K_s and K_b are the transmission coefficient from the surfactant and the blood to the lavage fluid, respectively. A_s and A_b are the effective surface area from the surfactant and the blood to the lavage fluid, respectively. The parameters m_l, m_s, and m_b represent the masses of protein in the lavage fluid, surfactant, and blood, respectively. V_l represents the fluid volume in lavage. V_s and V_b represent the fluid volume in surfactant and blood. We assumed that m_b, V_s, and V_b are constant during the WLL.

We calculated the temporal variation of the mass of protein and the volume of fluid in the stages of instilling, retaining, draining, and preparing in each lavage cycle, as described as follows.

Instilling stage. The volume change of protein and lavage fluid in the lung is expressed as:

$$\frac{dm_{in-out}}{dt} = 0 \quad (4)$$

$$\frac{dV_l}{dt} = \frac{dV_{in}}{dt} - \frac{dV_{l-b}}{dt} \quad (5)$$

where V_{in} is the fluid volume of instilled saline, and V_{l-b} is the fluid volume absorbed into the circulation expressed as

$$\frac{dV_{l-b}}{dt} = A_b \cdot R_{cl} \quad (6)$$

where R_{cl} is the absorption rate of fluid into the circulation. The concentration of protein was calculated as the ratio of the mass of protein to the fluid volume calculated from *Eqs. 1–6* according to the procedures described in the following subsection.

Retaining stage. No saline is instilling in the retaining stage, which means

$$\frac{dV_{in}}{dt} = 0 \quad (7)$$

The variation of the mass of protein and the volume of fluid were calculated from *Eqs. 1–7*.

Draining stage. The lavage fluid is drained in this stage, which means

$$\frac{dm_{in-out}}{dt} = -\frac{dm_{out}}{dt} \quad (8)$$

$$\frac{dV_l}{dt} = -\frac{dV_{out}}{dt} - \frac{dV_{l-b}}{dt} \quad (9)$$

where m_{out} and V_{out} are the protein mass and the fluid volume of drainage. The variation of the mass of protein and the volume of fluid were calculated from *Eqs. 1–3* and *6*, *8*, and *9*.

Preparing stage. Substance transfer in this stage may be considered to be similar to that in the retaining stage.

Data Processing and Statistics

Data including patient identity, protein concentrations in the serum or in the BALF of the right and left lungs, vital capacity, the number of cycles, the volume of instilled saline or drained lavage fluid, and time for each lavage stage were entered into a file (Microsoft Excel 2010). Using theoretical equations that solved protein concentrations in the drained lavage fluid (described in RESULTS), we wrote a program using Visual Basic Application to calculate the theoretical concentrations of proteins on the basis of specific variables.

Estimation of the protein concentration in the drained lavage fluid was carried out by numerically integrating differential equations using the following parameters: the volume of instilled saline, drained lavage fluid, time of each stage, the concentration of proteins in the first lavage cycle, effective alveolar and capillary surface area described below, and a given set of transmission coefficients, K_s and K_b. The resulting concentration curve was optimized with actual measurements manually by changing transmission coefficients. The effective areas of alveolar surface and pulmonary capillaries were calculated according to the equations described in Appendix A (10).

Numerical data were evaluated for normal distribution by using Shapiro-Wilk tests. Nonparametric data were analyzed by using Kruskal-Wallis rank sum test. Multiple comparisons were performed through a Bonferroni-adjusted Wilcoxon rank-sum test. All tests were two-sided, and P values <0.05 were considered statistically significant. Data were analyzed by using R-version 2.15.2 (R Foundation for Statistical Computing, Vienna, Austria).

RESULTS

Demographic and Clinical Findings for Study Subjects

Nine patients with active aPAP were enrolled in this study. Demographic data are shown in Table 1.

The mean age at WLL was 54.3 ± 11.4 yr old, with a male-to-female ratio of 2:1. The duration of the disease from onset was variable, ranging 10–96 mo. Patients showed no evidence of active pulmonary infection. Pulmonary functions and laboratory findings are described in Table 2.

The mean arterial oxygen pressure at room air was 64.0 ± 15.4 mmHg in seven patients and 55.2 and 67.4 mmHg for two patients under nasal oxygen supply. Percentage of vital capacity and percentage of carbon monoxide diffusing capacity were moderately to severely suppressed with 72.1 ± 17.7% and 51.0 ± 21.5%, respectively, whereas forced expiratory volume in 1 s/forced vital capacity was relatively conserved with 85.8 ± 10.9%. The mean serum biomarker levels of Krebs von den Lungen-6, SP-D, and carcinoembryonic antigen were 20,720 ± 13,953 IU/ml, 471 ± 271 ng/ml, and 26.7 ± 22.9 ng/ml, respectively. The mean serum GM-CSF autoantibody levels were 45.8 ± 51.7 μg/ml. These patient characteristics were similar to a past large Japanese cohort with PAP (17).

Timetables and Volume Balance for WLL

As shown in Fig. 1, *A* and *B*, each lavage cycle consisted of four stages: instilling (from the beginning to the end of saline instillation), retaining (from the end of saline instillation until the beginning of drainage), draining (from the beginning until the end of drainage), and preparing (from the end of drainage until the beginning of the next saline instillation). Twelve lungs from seven patients underwent WLL with short-term cycles (210–285 s), whereas five lungs from three patients underwent WLL with long-term cycles (550–634 s) (Table 3). In eight patients, both lungs underwent WLL; however, for one patient, only the right lung underwent lavage. Data for instilled saline volume, discharged lavage fluid volume, and time for each of the stages as defined above are shown in Tables 3 and 4. Lavage was repeated 11 to 29 times (median of 20 cycles) until the lavage fluid appeared clearer (Fig. 1*C*).

Time required for total WLL time ranged from 5,200 to 11,796 s. Instilling, retaining, draining, and preparing time